Acta Mechanica Slovaca **27 (4): 36 - 41,** December **2023**
https://doi.org/10.21496/ams.2023.035

Acta Mechanica Slovaca
ISSN 1335-2393
www.actamechanica.sk

Design of a Low-pressure Metal Hydride Reactor Designed for Hydralloy C5

Ivan Mihálik [1*], Filip Duda [1], Šimon Hudák [1], Natália Jasminská [1], Marián Lázár [1]

[1] Technical University of Košice, Faculty of Mechanical Engineering, Department of Power Engineering, Vysokoškolská 4, 042 00 Košice

Abstract: In this article, individual options for the implementation of hydrogen storage systems in vehicles are analysed. In particular, the conventional methods are described and hydrogen storage systems that use metal hydride alloys are discussed. The article presents the design of a low-pressure pressure vessel with a maximum operating pressure of 3MPa, compliant with the STN EN 13322-2 requirements. The newly-designed metal hydride pressure vessel was subjected to a strength analysis in the Ansys Static Structural environment at a maximum test hydraulic pressure of 4.7MPa. The measurement data describing the amount of the stored hydrogen which was obtained during the process of the activation of Hydralloy C5 is also analysed. The analysis included three cycles of hydrogen absorption and desorption.

Keywords: Hydrogen storage, metal hydride, strength analysis, finite element method.

1. Introduction

The development of safe and at the same time efficient forms of hydrogen storage is crucial for the successful development of the hydrogen economy. A low volumetric energy density of hydrogen appears to be particularly problematic, and represents a challenge in terms of the ability to store hydrogen in vehicles in a quantity that is sufficient to ensure the desired range [1]. Currently, in the case of passenger vehicles, the most frequently applied hydrogen storage method involves the use of pressure vessels with a maximum operating pressure of 70MPa. For trucks and buses, the maximum pressure of the hydrogen pressure vessels is 35MPa. A higher pressure in a pressure vessel facilitates a higher volumetric energy density. Such pressure vessels are typically made of steel; however, in order to reduce the weight, pressure vessels made of carbon fibres and reinforced with aluminium, steel or polymers are increasingly being used [2].

Another option is to store hydrogen in a liquid form at temperatures below 20K. In the case of using cryogenic tanks, the volumetric energy density of hydrogen is higher than that of hydrogen compressed to a pressure of 70MPa. However, the disadvantages associated with this option include the necessity to use highly-efficient thermal insulation for the pressure vessel, as well as the high total energy demand of the hydrogen liquefaction process [3].

The current research is increasingly focusing on hydrogen storage systems that use metal hydrides. In particular, among the known hydrogen storage methods, the use of metal hydrides facilitates achieving the highest volumetric density of energy [4]. It is also a safer storage method in terms of operating pressures. In order to enable the release of hydrogen, it is necessary to supply thermal energy to the metal hydride to reduce the risk of accidental hydrogen leaks. On the other hand, in order to ensure fast refilling of the hydrogen, the alloy must be cooled. It is therefore necessary to implement a system for the thermal management of low-pressure metal hydride pressure vessels.

*** Corresponding author:** Ivan Mihálik, ***E-mail address:*** *ivan.mihalik@tuke.sk*

2. Basic description of the designed pressure vessel for hydrogen storage

The design was created in compliance with STN EN 13322-2 [5], laying down the specifications for transportable refillable steel gas cylinders. This European standard describes the minimum requirements for certain aspects concerning the material, design, construction and workmanship, procedure and tests during the manufacture of transportable welded stainless steel gas cylinders with water capacities ranging from 0.5 l up to and including 150 l. The standard only applies to tanks made of stainless steel with a maximum tensile strength of less than $1{,}100 \cdot 10^6$ Pa. The newly-designed tank is a double-shell tank; it consists of the primary tank, in which the TiFe-based Hydralloy® is contained, and the outer shell.

The process of hydrogen absorption into the structure of a metal hydride alloy is an exothermic reaction, during which thermal energy is generated [6, 7]. It is therefore necessary to provide efficient cooling of the tank while it is in operation. The annulus between the primary tank and the outer shell is the space where a cooling fluid flows. This is the active cooling module for cooling the metal hydride alloy during the hydrogen absorption process. The material used in the production of the designed double-shell pressure vessel is the 316L/1.4404 stainless steel. The basic parameters of this material, which are necessary to calculate the basic strength characteristics of the designed pressure vessel, are listed in Table 1.

Table 1: Basic parameters of the 316L/1.4404 stainless steel for the calculations of strength characteristics

0.2% Re (MPa)	*Rm (MPa)*	*ρ (kg·m-3)*	*μ*	*E (MPa)*
200	500–700	8,000	0.3	$2.1 \cdot 10^5$

wherein *Re* is the offset yield strength (MPa); *Rm* – tensile strength (MPa); *ρ* – density (kg·m^3); μ – Poisson's ratio (-); and *E* – Young's modulus of elasticity (MPa).

The problematic heat transfer in powder alloys is rather significantly complicated by the efficient cooling and heating of the alloy across the pressure vessel volume [8, 9]. Therefore, the primary tank contains a heat transfer intensifier, which acts as a passive cooling module, in order to improve the transfer of heat towards the inner wall of the primary tank while the pressure vessel is being filled with hydrogen. The heat is efficiently removed by the cooling fluid flowing inside the annulus. The designed heat transfer intensifier consists of 8 primary and 8 secondary fins. The gap between the intensifier and the primary tank is 1 mm. The material from which the intensifier was made is aluminum (AlMg3), since it exhibits an optimal thermal conductivity (237 W·m^{-1}·K^{-1}) [10]. Fig. 1 shows the design of the pressure vessel and the newly designed shape of the internal heat transfer intensifier.

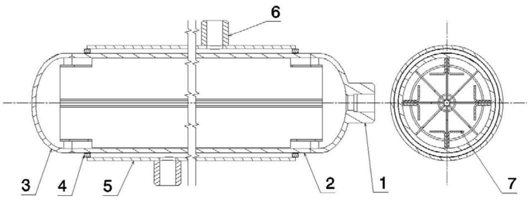

Figure 1: Design of the hydrogen storage pressure vessel. 1 – collar with the 1/4"NPT thread; 2 –cylindrical part of the primary tank; 3 – elliptical bottom; 4 – flange for the outer shell; 5 – cylindrical part of the outer shell with the cooling fluid; 6 – G1/2 flange; 7 – internal heat transfer intensifier.

3. Design of the pressure vessel for hydrogen storage

According to STN EN 13322-2, it was necessary to choose an optimal bottom for closing the tank. The standard prescribes two types of bottoms -torispherical and elliptical. The elliptical shape of the bottom was chosen for the design presented herein. It was also necessary to determine optimal thicknesses for the primary tank and the outer shell. They were calculated using the following equation:

wherein *a* is the calculated minimum thickness

$$a = \frac{D}{2} \cdot \left(1 - \sqrt{\frac{10 \cdot F \cdot J \cdot R_e - \sqrt{3} \cdot p_h}{10 \cdot F \cdot J \cdot R_e}}\right)(mm) \qquad (1)$$

of the primary tank/outer shell (mm); *J* – stress reduction factor (-); *F* – design value of the stress factor (-); *Re* – calculated offset yield strength of the selected material (MPa); and p_h – test hydraulic pressure above the atmospheric pressure (bar).

The pressure vessel was designed to contain the primary tank with a diameter of 60.3 mm. Based on Annex A to STN EN 13322-2, the stress reduction factor *J* was 1 since the butt weld of the closure was considered. The design value of the stress factor *F* was 0.77, as prescribed by the standard.

For the purpose of calculating the minimum thickness, the value of offset yield strength Re was limited to a maximum of 0.85·*Rg*. The calculated offset yield strength value was 425MPa and the ultimate tensile strength of the 1.4404 steel was 500MPa.

The chosen value of the test hydraulic pressure above the atmospheric pressure was 47 bar. This value represents the maximum test pressure, and it was identified on the basis of STN EN 13445-5, Section 10.2.2.3 Standard Hydraulic Testing. The standard specifies that the test pressure must not be lower than the value calculated using the following equation:

$$p_h = 1.43 \cdot p_t \left(Pa \right) \tag{2}$$

where pt is the operating pressure of $30 \cdot 10^5$ (Pa).

After substituting the value of the operating pressure into Equation (2), the resulting value of the test pressure was 43·105Pa. Based on the calculation of the thickness, which was made using Equation (1), the calculated value of the minimum thickness of the cylindrical part of the primary tank was 0.1mm, while the thickness of the outer shell was 0.05mm.

Section 5.4.1 of STN EN 13322-2 specifies the absolute minimum for the thickness of bottoms and of the cylindrical parts of the designed pressure vessel, while applying the requirements (3–5):

Since the diameter of the designed pressure vessel is smaller than 100 mm, the selected minimum thicknesses of the cylindrical parts of the primary tank and of the outer shell had to be larger than or equal 1.1mm because the thicknesses calculated using Equation (1) were much smaller. The standard also states that all welds must be visually controllable. That is why the cylindrical part of the primary tank must be seamless. Table 2 contains the selected dimensions of the cylindrical parts and of the bottoms of the designed pressure vessel.

Table 2: Selected dimensions of the cylindrical parts and of the bottoms of the metal hydride pressure vessel

	a (mm)	*b (mm)*	*a2 (mm)*	*h (mm)*	*H (mm)*
Selected dimensions	2.6	2.6	2	5	20

wherein a is the selected thickness of the cylindrical part of the primary tank; b–selected thickness of the elliptical bottom; a2–selected thickness of the cylindrical part of the outer shell; h–selected height of the cylindrical part of the bottom; and H–selected external height of the arched part of the bottom.

4. Strength calculation for the designed pressure vessel for hydrogen storage

The analysed pressure vessel was subdivided into n finite elements. The grid of finite elements consisted of approximately 100,000 volumetric finite elements with the quadratic approximation and 240,000 grid points. The strength calculation was made using the basic parameters of the stainless steel material (Table 1).

The next step of the simulation was the creation of the boundary conditions [11, 12]. The boundary conditions that were applied to the analysed model are summarised in the following outline:

– *The force acting on the surface of the tank wall, determined by the weight of the powder metal hydride, is replaced with the equivalent action of the hydrostatic pressure of the fictive fluid of the same density of 7,000kg·m^{-3}.*

– *The pressure on the inner surfaces of the analysed pressure vessel is defined as the maximum test hydraulic pressure of 4.7MPa.*

– *The pressure on the outer walls of the pressure vessel is defined as the value of 0.5MPa.*

– *The surfaces that are in contact with the cooling fluid are subject to the requirement of the hydrostatic pressure and a density of 1,000kg·m^{-3}.*

– *The self-weight of the metal hydride pressure vessel is also applied.*

– *The width of the surface area onto which the cylindrical bond is applied is 20 mm and its perimeter corresponds to the size of the metal hydride pressure vessel. The bond near the valve of the pressure vessel has the radial and axial displacements removed, while the bond near the closed end of the pressure vessel has the degrees of freedom removed in the radial direction only.*

– *The considered temperature is 60°C, i.e. the boundary temperature at which the metal hydride alloy (Hydralloy) is capable of absorbing hydrogen into its structure.*

Results of the strength simulation are shown in Table 3 and Fig. 2:

$$D \le 100mm, a = b = 1.1mm \tag{3}$$

$$100mm < D \le 150mm, a = b = 1.1 + 0.008 \cdot \left(D - 100 \right) mm \tag{4}$$

$$D \ge 150mm, a = b = \frac{D}{250} + 0,7 \left(with\ the\ absolute\ \min ium\ of\ 1.5mm \right) \tag{5}$$

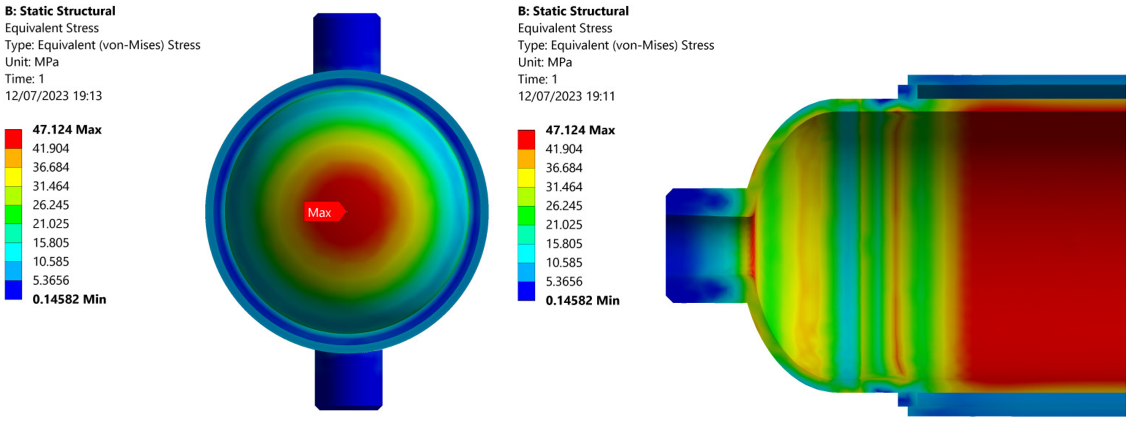

Figure 2: Results of the strength simulation at the internal pressure of 4.7MPa

Table 3: Resulting values of the searched parameters of the metal hydride pressure vessel at the internal pressure of 4.7MPa

Total displacement	0.16 mm
Displacement along the x-axis	0.005 mm
Displacement along the z-axis	0.13 mm
Von Mises stress	47.124 MPa

The results of the simulation clearly showed that the pressure vessel designed in compliance with the STN EN 13322-2 standard meets the requirements for operating parameters, since the von Mises stress did not reach the values of the offset yield strength of the selected material at the hydraulic pressure of 4.7MPa.

5. Comparison of the amount of hydrogen stored in the pressure vessel during the individual cycles of the Hydralloy C5 activation

Prior to the measurements, the pressure vessel was filled with 5.4 kg of the metal hydride alloy (Hydralloy C5). For the purpose of quantifying the free volume between the grains of the powder alloy inside the pressure vessel, an inert gas (argon) was used. Following the quantification of the free volume, the pressure vessel was vacuumed with a vacuum pump for 30 minutes in order to completely remove argon from the free volume inside the pressure vessel. The subsequent process of the alloy activation consisted of 3 cycles of hydrogen absorption and desorption. The first absorption cycle, shown in Fig.3, lasted for 5,000 seconds. During the cycle, 71.62 l of hydrogen were stored in the pressure vessel. Fig.3 shows that the absorption of hydrogen into the alloy significantly decelerated after approximately 4,600 seconds; this resulted in the gradual stabilisation of the pressure and of the total amount of the hydrogen stored in the pressure vessel.

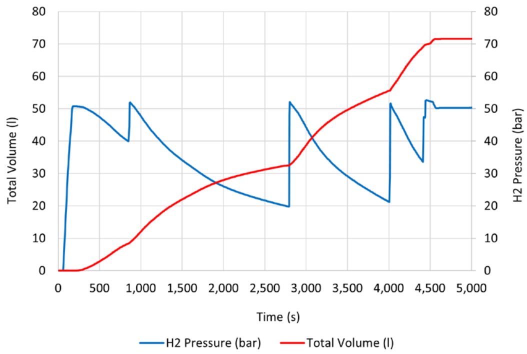

Figure 3: Alloy activation – first absorption cycle

The graph shows that the total stored amount of hydrogen increased in 5 sections, during which the pressure in the system increased due to the opening of the reducing valve of the hydrogen pressure vessel, which was aimed at increasing the flow rate of hydrogen flowing into the low-pressure pressure vessel. As may be seen in the figure, the individual sections show a pressure drop, during which hydrogen was absorbed into the alloy. The pressure drop was gradually decelerating while the hydrogen flow rate was gradually decreasing; this resulted in a decelerated increase in the total volume of hydrogen in the pressure vessel, which lasted until the pressure was increased again. After the first absorption cycle, the hydrogen was released from the system into the atmosphere. Subsequently, the pressure vessel was vacuumed for 60 minutes with a vacuum pump.

In the second absorption cycle (Fig. 4), 537.936 l of hydrogen was stored in the pressure vessel over the period of 10,000 seconds. During the second measurement, the pressure in the system was maintained at 50 bar for the first 5,400 seconds, which resulted in only a slight decrease in the hydrogen flow rate, and hence a smoother increase in the total volume of the stored hydrogen. Subsequently, after the reducing valve of the hydrogen pressure vessel was closed, the pressure in the system decreased while the hydrogen was being absorbed into the alloy from the free volume. After the reducing valve was closed and the pressure decreased, the absorption process significantly decelerated and only 0.175 l of hydrogen was absorbed into the alloy over the period of last 4,600 seconds.

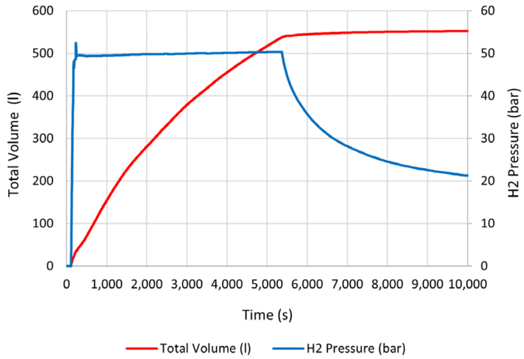

Figure 4: Alloy activation – second absorption cycle

After the second absorption cycle was completed and the hydrogen was released from the system, the system was vacuumed for 180 minutes. The third cycle of hydrogen absorption into the alloy (Fig. 5) lasted for 6,832 seconds, while the pressure vessel was capable of storing in total 985.63 l of hydrogen. Over the period of 2,800 seconds, the pressure was smoothly regulated in order to maintain the approximately constant flow rate of hydrogen flowing into the pressure vessel; this resulted in a linear increase in the volume of hydrogen stored in the pressure vessel. After the period of 2,800 seconds elapsed and the pressure of ca 50 bar was achieved, the hydrogen flow rate gradually decreased while the constant pressure was maintained. At the same time, the total increase in the volume of hydrogen in the pressure vessel decelerated. After the period of 5,350 seconds, the reducing valve of the pressure vessel was closed and the pressure decreased. During the pressure decrease, hydrogen was absorbed into the alloy from the free volume.

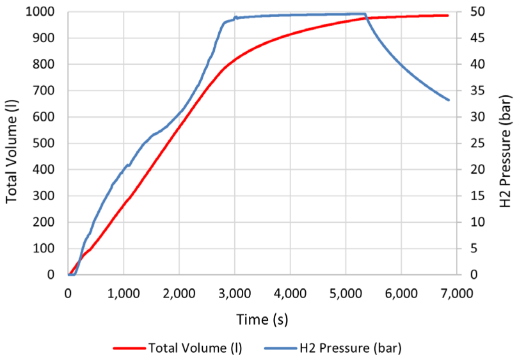

Figure 5: Alloy activation – third absorption cycle

6. Conclusions

The low-pressure metal hydride pressure vessel was designed in compliance with the requirements laid down in the STN EN 13322-2 standard on design and construction of refillable steel gas cylinders. The necessity of implementing a thermal management system was addressed through the utilisation of the annulus between the outer shell and the wall of the primary tank for the cooling fluid flow and the design of the internal heat transfer intensifier. The final design of the pressure vessel was subjected to the strength analysis carried out in the Ansys Static Structural environment by applying the final element method. Based on the results of the numerical simulation, it may be stated that the presented design of the pressure vessel meets the requirements for the operating and strength parameters, since the values of the maximum von Mises stress, at the maximum test hydraulic pressure, were more than 4-times lower than the offset yield strength of the used material.

The designed and constructed pressure vessel was also used in the experimental process of activation of Hydralloy C5. Results of the measurements that were carried out during the 3 individual cycles of hydrogen absorption indicated that at the beginning of the process the alloy can absorb only a small amount of hydrogen into its structure. During the second and third absorption cycles, the total amount of the hydrogen stored in the alloy significantly increased. This phenomenon is caused by the formation of tiny cracks in the alloy grains during the absorption and desorption processes. Such cracks lead to the disintegration of the alloy powder grains into even smaller microparticles, and this subsequently contributes to a faster absorption of a larger amount of hydrogen into the metal hydride alloy.

Acknowledgments: This paper was written with the financial support from the VEGA granting agency within the Projects No. 1/0224/23 and No. 1/0532/22, from the KEGA granting agency within the Project No. 012TUKE-4/2022, and with the financial support from the APVV granting agency within the Projects No. APVV-15-0202, APVV-20-0205 and APVV-21-0274.

References

[1.] Sundén, B. (2019). Chapter 3 – Hydrogen. Bengt Sundén, Hydrogen, Batteries and Fuel Cells. Academic Press, pages 37-55. ISBN 978-0-12-816950-6

[2.] Folkson, R. (2022). 6 – Hydrogen as an energy vector for transportation vehicles. Richard Folkson, Steve Sapsford, Alternative Fuels and Advanced Vehicle Technologies for Improved Environmental Performance (Second Edition). Woodhead Publishing, pages 151-171. ISBN 978-0-323-90979-2

[3.] Wan, Ch. et al (2023). Numerical Simulation on Pressure Evolution Process of Liquid Hydrogen Storage Tank with Active Cryogenic Cooling: Simulation numérique du processus d'évolution de pression du réservoir de stockage d'hydrogène liquid avec refroidissement cryogénique actif. In: International Journal of Refrigeration, DOI: https://doi.org/10.1016/j.ijrefrig.2023.01.012

[4.] Desai, F. J. et al (2023). A critical review on improving hydrogen storage properties of metal hydride via nanostructuring and integrating carbonaceous materials. In: International Journal of Hydrogen Energy, DOI: https://doi.org/10.1016/j.ijhydene.2023.04.029

[5.] STN EN 13322-2 (2003). Prepravné fľaše na plyny. Navrhovanie a výroba znovuplniteľných oceľových fliaš na plyny. Časť 2: Nehrdzavejúce ocele, 2003

[6.] Lototskyy, M. V. et al (2016). Performance of electric forklift with low-temperature polymer exchange membrane fuel cell power module and metal hydride hydrogen storage extension tank. In: Journal of Power Sources, volume 316, pages 239-250. DOI: https://doi.org/10.1016/j.jpowsour.2016.03.058

[7.] Krishna, K. V. et al (2022). Bio-inspired leaf-vein type fins for performance enhancement of metal hydride reactors. In: International Journal of Hydrogen Energy, volume 47, issue 56, pages 23694-23709. DOI: https://doi.org/10.1016/j.ijhydene.2022.05.163

[8.] Dunikov, D. O. et al (2023). Permeability of a deformable metal hydride bed during hydrogen absorption. In: International Journal of Hydrogen Energy, DOI: https://doi.org/10.1016/j.ijhydene.2023.05.224

[9.] Zhang, T. et al (2005). A Review of Heat Transfer Issues in Hydrogen Storage Technologies. In: ASME Journal of Heat and Mass Transfer, volume 127, issue 12, pages 1391-1399. DOI: https://doi.org/10.1115/1.2098875

[10.] Zhang, A., Li, Y. (2023). Thermal Conductivity of Aluminium Alloys – A Review. In: Materials (Basel), volume 16, issue 8. DOI: https://doi.org/10.3390/ma16082972

[11.] Bocko, J. et al (2019). Simulácia v programe ANSYS. Technická univerzita v Košiciach, Strojnícka fakulta, 172 pages. ISBN: 978-80-553-3335-9

[12.] Matej, J. et al (2015). Simulácia virtuálnych prototypov - napäťovo-deformačné analýzy. Technická univerzita vo Zvolene, 148 pages. ISBN: 978-80-228-2828-4